

X-ray dichroism in biaxial gyrotropic media: Differential absorption and fluorescence excitation spectra

J. Goulon^{1,a}, C. Goulon-Ginet^{1,b}, A. Rogalev¹, V. Gotte¹, C. Brouder², and C. Malgrange²

¹ European Synchrotron Radiation Facility, B.P. 220, 38043 Grenoble Cedex, France

² Laboratoire de Minéralogie Cristallographie^c, Universités Paris VI & VII, Tour 16, 4 place Jussieu, 75252 Paris Cedex 05, France

Received 3 March 1999

Abstract. The differential absorption and the differential change in the polarization state of an X-ray beam propagating inside a gyrotropic crystal are described using a 4×4 Müller matrix, the 16 elements of which are related to the anisotropic components of the multipolar polarizability tensors at the absorbing site. Analytical expressions are given up to third order for X-ray linear and circular dichroism, X-ray optical rotation and X-ray circular polarimetry in transmission. The same formalism is extended to discuss *Fluorescence detected dichroism* spectra with or without polarization analysis of the fluorescence. *Fluorescence detected dichroism* is strictly proportional to dichroism measured in the transmission geometry only for uniaxial crystals. In biaxial crystals, the tiny effects of X-ray gyrotropy are swamped by large linear dichroism signals due to the imperfect polarization transfer function of Bragg monochromators. Second order effects should also be taken into consideration. Our general formulation of linear and circular dichroism includes terms of *odd parity* with respect to the action of the time reversal operator: such terms cannot contribute to *natural* dichroism but can be activated by a magnetic field. The terms responsible for X-ray magnetic circular dichroism are well known but *non-reciprocal* X-ray gyrotropy effects are also predicted in magnetic crystals of appropriate symmetry.

PACS. 33.55.Ad Optical activity, optical rotation; circular dichroism – 41.50.+h X-ray beams and X-ray optics – 78.70.Dm X-ray absorption spectra

1 Introduction

We have produced recently the very first unambiguous experimental evidence [1] of **F**luorescence **d**etected **X**-ray **N**atural **C**ircular **D**ichroism (Fd-XNCD) in a uniaxial gyrotropic crystal of lithium iodate (α -LiIO₃), *i.e.* a crystal known to exhibit a large specific rotativity together with a very strong non-linear susceptibility in the visible range. With such thick and heavily absorbing crystals, dichroism experiments can hardly be performed in transmission and it is much simpler to record differential X-ray fluorescence excitation spectra using an incident X-ray beam which is either right - or left - circularly polarized. Of course, in the case of a uniaxial crystal such as α -LiIO₃, it is preferable to keep the direction of the incident X-ray beam colinear with the optical axis of the crystal. The same geometry was retained to detect Fd-XNCD in a pair of enantiomeric crystals of a stereogenic organometallic complex in which the absorbing metal center was sitting in

a chiral ligand field [2]. In both experiments, the origin of XNCD was assigned to electric dipole - electric quadrupole ($E_1.E_2$) interference terms which contribute to the pseudoscalar part of the optical activity tensor. A theory of XNCD has been developed in the framework of multiple scattering (MS) and has been published in a previous issue of the same journal [3].

Unfortunately, one is running into serious complications as soon as the isotropy is lost in a plane perpendicular to the direction of propagation of the incident X-ray beam. It is well documented from classical optics that optical activity, linear dichroism and birefringence may occur all together in biaxial crystals and that the last two effects usually swamp completely those of gyrotropy: very sophisticated experimental techniques are then required to disentangle what is truly due to gyrotropy in a CD experiment. On the other hand, light propagating inside a biaxial crystal does not keep a constant polarization state [4]. Since this point was systematically neglected in all previous X-ray studies on oriented crystals [5,6], we found attractive to analyze carefully what is really measured when a polarized X-ray beam propagates inside a biaxial, gyrotropic crystal. Recall that a somewhat mysterious “*X-ray crystal optics effect*” was predicted to

^a e-mail: goulon@esrf.fr

^b *also:* Université de Grenoble-I, Faculté de Pharmacie, 38706 La Tronche, France

^c CNRS URA9

occur in all biaxial crystals [7]: the origin of this second order effect will become fully transparent from our analysis. It has also the practical consequence that *fluorescence detected* dichroism spectra cannot be anymore rigorously equivalent to dichroism spectra recorded in a transmission geometry. Nevertheless, we like to point out that complementary information could be extracted from a detailed analysis of the polarization components of the X-ray fluorescence photons emitted in a given direction.

The organization of the paper is the following: in Section 2, the differential absorption and the differential change in the polarization state of the X-ray beam are described using a 4×4 Müller matrix, the 16 elements of which are related to the anisotropic components of the multipolar polarizability tensors at the absorbing site. We propose analytical expressions of the Stokes components at any point along the propagation axis of the X-ray beam inside the crystal. In Section 3, we derive general formula for X-ray Circular Dichroism (XCD), X-ray Linear Dichroism (XLD), X-ray Optical Rotation (XOR), X-ray Circular Polarimetry (XCP) for a transmission geometry. In Section 4, the same formalism is extended to calculate Fd-XCD spectra with (or without) polarization analysis. Finally, we discuss in Section 5 the consistency of all our results with respect to symmetry, rotational invariance and time reversality properties and we briefly review what are the implications regarding magnetic crystals.

2 Stokes vector in anisotropic absorbing media

Let us consider a quasi monochromatic X-ray beam propagating along the z direction through a crystal plate of finite thickness d and which is infinitely wide in the $\{x, y\}$ plane. As a first step, we wish to describe the differential absorption and the differential change of polarization induced by a thin layer of infinitesimal thickness dz .

2.1 Differential Müller equation

We found most convenient to extend into the X-ray range the theory of refringent scattering which was elaborated by Buckingham *et al.* [8–10] for optical spectroscopy. Recall that an important implication of this theory is that all modes propagating inside the crystal should be parallel to the wave vector of the incident beam: this requirement is quite acceptable in the X-ray range where the real part of the refractive index $n = 1 - \delta$ is very close to unity ($\delta \leq 10^{-5}$) with the practical consequence that critical angles for X-ray reflection $\theta_c = \sqrt{2\delta}$ are in the range of a few mrad. Thus, for a transverse polarized wave propagating along the direction \mathbf{n} , the complex *scattering tensor* $a_{\alpha\beta}^*$ can reasonably be expanded as:

$$a_{\alpha\beta}^* = \alpha_{\alpha\beta}^* + \zeta_{\alpha\beta\gamma}^* \mathbf{n}_\gamma + Q_{\alpha\gamma\beta}^* [\mathbf{n}_\gamma^2] + \dots \quad (1)$$

where: $\alpha, \beta \neq \gamma$. In equation (1), $\alpha_{\alpha\beta}^*$ and $Q_{\alpha\gamma\beta}^*$ are respectively the complex *electric dipole* polarizability tensor and the complex *electric quadrupole* polarizability

tensor, the detailed expressions of which are given in Appendix A1. There have been ample experimental evidence produced in these recent years [5, 11–15] that X-ray absorption spectroscopy is sensitive to the electric quadrupole ($E_2.E_2$) cross sections: this implies that the last term of equation (1) should not be neglected in the X-ray range. It is precisely the aim of this paper to show that the complex *Gyrotropy* tensor $\zeta_{\alpha\beta\gamma}^*$, which is written in full detail in Appendix A1, can also play a significant role in X-ray absorption or excitation spectroscopies.

For biaxial crystals which are anisotropic in a plane perpendicular to the direction of propagation (0, 0, 1), it is most appropriate to introduce the following complex tensors:

$$t^* = t - it' \\ = [\alpha_{xx}^* + \alpha_{yy}^*] + [\zeta_{xxz}^* + \zeta_{yyz}^*] + [Q_{xzzx}^* + Q_{yzzx}^*] \quad (2)$$

$$u^* = u - iu' \\ = [\alpha_{xx}^* - \alpha_{yy}^*] + [\zeta_{xxz}^* - \zeta_{yyz}^*] + [Q_{xzzx}^* - Q_{yzzx}^*] \quad (3)$$

$$v^* = v - iv' \\ = [\alpha_{xy}^* + \alpha_{yx}^*] + [\zeta_{xyz}^* + \zeta_{yxz}^*] + [Q_{xzzx}^* + Q_{yzzx}^*] \quad (4)$$

$$w^* = w - iw' \\ = [\alpha_{xy}^* - \alpha_{yx}^*] + [\zeta_{xyz}^* - \zeta_{yxz}^*] + [Q_{xzzx}^* - Q_{yzzx}^*] \quad (5)$$

and by direct identification, one obtains:

$$t = + [\alpha_{xx}(f) + \alpha_{yy}(f)] + [\zeta_{xxz}(f) + \zeta_{yyz}(f)] \\ + [Q_{xzzx}(f) + Q_{yzzx}(f)] \quad (6)$$

$$t' = - [\alpha_{xx}(g) + \alpha_{yy}(g)] - [\zeta_{xxz}(g) + \zeta_{yyz}(g)] \\ - [Q_{xzzx}(g) + Q_{yzzx}(g)] \quad (7)$$

$$u = + [\alpha_{xx}(f) - \alpha_{yy}(f)] + [\zeta_{xxz}(f) - \zeta_{yyz}(f)] \\ + [Q_{xzzx}(f) - Q_{yzzx}(f)] \quad (8)$$

$$u' = - [\alpha_{xx}(g) - \alpha_{yy}(g)] - [\zeta_{xxz}(g) - \zeta_{yyz}(g)] \\ - [Q_{xzzx}(g) - Q_{yzzx}(g)] \quad (9)$$

$$v = +2 [\alpha_{xy}(f) + \zeta_{xyz}(f) + Q_{xzzx}(f)] \quad (10)$$

$$v' = -2 [\alpha_{xy}(g) + \zeta_{xyz}(g) + Q_{xzzx}(g)] \quad (11)$$

$$w = +2 [\alpha'_{xy}(g) + \zeta'_{xyz}(g) + Q'_{xzzx}(g)] \quad (12)$$

$$w' = -2 [\alpha'_{xy}(f) + \zeta'_{xyz}(f) + Q'_{xzzx}(f)]. \quad (13)$$

As detailed in Appendix A1, f and g refer to the *dispersive* and *absorptive* lineshapes respectively. It will appear in the following sections that, for biaxial crystals, the quantity $[uv' - vu']$ will play an important role. It could be easily checked on starting from the various definitions found in Appendix A1 that, due to the summation over all excited states, we have *a priori*: $[uv' - vu'] \neq 0$.

Barron [4] has clearly established that the variation of the Stokes vector $|\mathbf{S}(z)\rangle$ of any incident beam as a function of its penetration depth z is given by a linear differential

equation of the type:

$$\frac{\partial}{\partial z} |\mathbf{S}(z)\rangle = a [\mathbf{M}] \cdot |\mathbf{S}(z)\rangle \quad (14)$$

in which: $a = (1/2)\omega N\mu_0 c$, μ_0 being the permeability of free space and N the number density of absorbing centers [4]. The matrix $[\mathbf{M}]$ can be identified with a *differential* Müller matrix to be written:

$$[\mathbf{M}] = \begin{bmatrix} t' & u' & -v' & w \\ u' & t' & -w' & v \\ -v' & w' & t' & u \\ w & -v & -u & t' \end{bmatrix}. \quad (15)$$

This is the point at which we deviate from the earlier analysis by Barron [4] since he converted immediately the four Stokes parameters into physically relevant quantities, *i.e.* the beam intensity I , the azimuth ϑ , the ellipticity η and the degree of polarization P_d using classical definitions:

$$I = \frac{1}{2} \left[\frac{\varepsilon\varepsilon_0}{\mu\mu_0} \right]^{1/2} S_0 \quad (16)$$

$$\vartheta = \frac{1}{2} \arctan \left[\frac{S_2}{S_1} \right] \quad (17)$$

$$\eta = \frac{1}{2} \arctan \left[\frac{S_3}{\sqrt{S_1^2 + S_2^2}} \right] \quad (18)$$

$$P_d = \frac{[S_1^2 + S_2^2 + S_3^2]^{1/2}}{S_0}. \quad (19)$$

The problem with the latter transformation is that the set of coupled differential equations replacing equation (14) is not anymore linear and the integration becomes intractable except for uniaxial crystals. Our own strategy was to integrate first equation (14).

2.2 Integrated Müller matrix $[\Phi(\mathbf{z})]$

2.2.1 Uniaxial gyrotropic crystals

For a uniaxial gyrotropic crystal aligned in such a way that the optical axis coincides with the direction of propagation of the X-ray beam, the differential Müller matrix (15) simplifies a lot since $u = u' = v = v' = 0$:

$$[\mathbf{M}] = \begin{bmatrix} t' & 0 & 0 & w \\ 0 & t' & -w' & 0 \\ 0 & w' & t' & 0 \\ w & 0 & 0 & t' \end{bmatrix}. \quad (20)$$

The secular equation has the following roots:

$$\lambda_1 = t' - w; \quad \lambda_2 = t' + w; \quad \lambda_3 = t' - iw'; \quad \lambda_4 = t' + iw'$$

and admits the following eigenvectors:

$$\begin{aligned} \rho_1 &= \begin{bmatrix} 1/\sqrt{2} \\ 0 \\ 0 \\ -1/\sqrt{2} \end{bmatrix} & \rho_2 &= \begin{bmatrix} 1/\sqrt{2} \\ 0 \\ 0 \\ +1/\sqrt{2} \end{bmatrix} \\ \rho_3 &= \begin{bmatrix} 0 \\ 1/\sqrt{2} \\ i/\sqrt{2} \\ 0 \end{bmatrix} & \rho_4 &= \begin{bmatrix} 0 \\ i/\sqrt{2} \\ 1/\sqrt{2} \\ 0 \end{bmatrix}. \end{aligned} \quad (21)$$

A general solution to the differential equation (14) is:

$$|\mathbf{S}(z)\rangle = [\mathbf{R}_v] [\mathbf{D}_\lambda] [\mathbf{R}_v^{-1}] |\mathbf{S}^0\rangle \quad (22)$$

with the following definitions:

$$\begin{aligned} [\mathbf{R}_v] &= [\rho_1 \ \rho_2 \ \rho_3 \ \rho_4]; & |\mathbf{S}^0\rangle &= |\mathbf{S}(z=0)\rangle; \\ [\mathbf{D}_\lambda]_{ij} &= \delta_{ij} \exp(a\lambda_j z) \end{aligned}$$

δ_{ij} being the Kronecker symbol. Finally, the Stokes vector $|\mathbf{S}(z)\rangle = [\Phi(z)] |\mathbf{S}^0\rangle$ can be written:

$$\begin{aligned} \begin{bmatrix} S_0(z) \\ S_1(z) \\ S_2(z) \\ S_3(z) \end{bmatrix} &= \exp(at'z) \\ &\times \begin{bmatrix} \cosh(awz) & 0 & 0 & \sinh(awz) \\ 0 & \cos(aw'z) & -\sin(aw'z) & 0 \\ 0 & \sin(aw'z) & \cos(aw'z) & 0 \\ \sinh(awz) & 0 & 0 & \cosh(awz) \end{bmatrix} \begin{bmatrix} S_0^0 \\ S_1^0 \\ S_2^0 \\ S_3^0 \end{bmatrix}. \end{aligned} \quad (23)$$

2.2.2 Biaxial gyrotropic crystals

The first step is to solve a biquadratic secular equation of matrix $[\mathbf{M}]$:

$$[\lambda - t']^4 + P[\lambda - t']^2 - Q^2 = 0 \quad (24)$$

with:

$$\begin{aligned} P &= [u^2 - u'^2] + [v^2 - v'^2] - [w^2 - w'^2] \\ Q &= uu' + vv' - ww'. \end{aligned}$$

The eigenvalues of equation (24) can again be written:

$$\lambda_1 = t' - B'; \quad \lambda_2 = t' + B'; \quad \lambda_3 = t' - iA'; \quad \lambda_4 = t' + iA'$$

but analytical expressions for A' and B' are getting rather cumbersome. A solution to the differential equation (14) can still be given by equation (22) provided that one is able to develop analytically the eigenvector matrix $[\mathbf{R}_v]$ and its inverse $[\mathbf{R}_v^{-1}]$. Note that the final result can still be written:

$$|\mathbf{S}(z)\rangle = [\Phi(z)] |\mathbf{S}^0\rangle \quad (25)$$

with matrix elements $\varphi_{ij}(z)$ that have all the same functional form:

$$\varphi_{ij}(z) = \exp(at'z) \times \left\{ \begin{array}{l} \left[\frac{1}{2}\delta_{ij} + \beta_{ij}'' \right] \cos(aA'z) - \left[\gamma_{ij}' + \gamma_{ij}'' \right] \sin(aA'z) \\ + \left[\frac{1}{2}\delta_{ij} - \beta_{ij}'' \right] \cosh(aB'z) + \left[\gamma_{ij}' - \gamma_{ij}'' \right] \sinh(aB'z) \end{array} \right\}. \quad (26)$$

For practical applications, we need analytical expressions of the individual functions $\varphi_{ij}(z)$. As detailed in Appendix A2, one can save much algebra by defining complex matrices: $[\mathbf{M}^\pm] = [\mathbf{M}'] \pm i[\mathbf{M}'']$ where $[\mathbf{M}']$ and $[\mathbf{M}'']$ are traceless matrices. Matrix $[\Phi]$ can then be easily expanded as a series of successive powers in z .

3 X-ray dichroism and polarimetry in transmission

3.1 Circular dichroism

3.1.1 Formulation

Circular dichroism is the difference in the absorption cross sections measured during two consecutive experiments carried out with an incident light that is respectively left- and right-handed circularly polarized. For each experiment, the polarization state is characterized by the Stokes-Poincaré's ratios defined according to the following convention [4]:

$$P_1^0 = \frac{S_1^0}{S_0^0} = \frac{I_0^{90^\circ} - I_0^{0^\circ}}{I_0^{90^\circ} + I_0^{0^\circ}}; \quad P_2^0 = \frac{S_2^0}{S_0^0} = \frac{I_0^{45^\circ} - I_0^{135^\circ}}{I_0^{45^\circ} + I_0^{135^\circ}}$$

$$P_3^0 = \frac{S_3^0}{S_0^0} = \frac{I_0^R - I_0^L}{I_0^R + I_0^L}.$$

Of course, one would like to have two monochromatic beams of strictly opposite polarization state, *i.e.* $I_0 \{P_1^0 = P_2^0 = 0; P_3^0 = \pm 1\}$ and therefore:

$$[\sigma^L - \sigma^R] = \ln \left(\frac{[I^R/I_0^R]}{[I^L/I_0^L]} \right) = \ln \left(\frac{\phi_{00}(z) + \phi_{03}(z)}{\phi_{00}(z) - \phi_{03}(z)} \right)$$

$$= \ln \left(1 + \frac{2\xi_{03}(z)}{1 - \xi_{03}(z)} \right) \simeq 2\xi_{03} \quad (27)$$

where: $\xi_{0j}(z) = \phi_{0j}(z)/\phi_{00}(z)$. Unfortunately, such “*ideal conditions*” are never met in the X-ray range: even with a nearly perfect helical undulator source [16], one has still to worry about the polarization transfer function of the two-crystal monochromator which is getting very poor when the Bragg angle approaches 45° with the practical consequence that $P_1^0 \neq 0$ and is rapidly increasing [17]. Furthermore, flipping the helicity of the photons emitted by the source does not imply that the circular polarization

rate of the monochromatic X-ray beam is reversed since what is monitored downstream with respect to a two-crystal monochromator is a complicated change of polarization state [1]:

$$\{P_1^h, P_2^h, +P_3^h\}_{\text{Source}} \iff \{P_1^h, P_2^h, -P_3^h\}_{\text{Source}}$$

$$\Downarrow \text{[Monochromator]}$$

$$\{P_1^0, P_2^0, +P_3^0\} \iff \{P_1^0, P_2^0(1 - \varepsilon_2), -P_3^0(1 - \varepsilon_3)\}$$

where $\varepsilon_{2,3}$ become significant as soon as $P_2^0 \neq 0$ (which is most often the case...). Neglecting again the non linear terms with respect to ξ_{03} , the *apparent* circular dichroism has, in practice, to be reformulated as:

$$[\sigma^L - \sigma^R] \approx \frac{2\xi_{03}P_3^0(1 - \varepsilon_3)}{1 + \xi_{01}P_1^0 + \xi_{02}P_2^0} + \frac{\xi_{02}\varepsilon_2P_2^0}{1 + \xi_{01}P_1^0 + \xi_{02}P_2^0}. \quad (28)$$

Thus, in biaxial crystals, the *measured* circular dichroism is most often contaminated with unwanted *linear* dichroism due to the second term in equation (28). The latter is usually large enough to swamp completely the tiny contribution of gyrotropy. Note that the denominator may also induce a second order correction if the experiments are carried out with elliptically polarized photons.

3.1.2 Uniaxial crystals with the beam propagating along the optical axis

Since: $\phi_{01}(z) = \phi_{02}(z) = 0$, we have $\xi_{01}(z) = \xi_{02}(z) = 0$. As a consequence, *there cannot be any contamination by linear dichroism*. Furthermore, one directly obtains from (23): $\xi_{03}(z) = \tanh(awz)$ and, in full agreement with reference [4], the XCD signal is given by:

$$[\sigma^L - \sigma^R] \approx 2(awd)P_3^0(1 - \varepsilon_3/2) \quad (29)$$

where d is the crystal thickness.

3.1.3 Biaxial crystals

Let us first restrict our analysis to the simplest case of experiments performed under ideal conditions ($P_1^0 = P_2^0 = 0; P_3^0 = \pm 1$). Direct substitution of equation (27) with the series expansion detailed in Appendix A2 yields up to the third order:

$$[\sigma^L - \sigma^R] \approx \left\{ \begin{array}{l} 2(awd) - (ad)^2[uv' - vu'] \\ -\frac{1}{3}(ad)^3[w(u^2 + v^2 + 2u'^2 + 2v'^2) + w'(uu' + vv')] \end{array} \right\}. \quad (30)$$

The first order term of equation (30) is the same as for uniaxial crystals and characterizes the crystal gyrotropy. However, even under ideal conditions, *i.e. in the absence of unwanted linear dichroism*, there is a second order term

$$\Delta\vartheta(z) \approx \left\{ \begin{array}{l} -\frac{1}{2}ad(v'-w') + \frac{1}{4}(ad)^2[u'(v'-w')-u(v-w)] \\ +\frac{1}{12}(ad)^3 \left[\begin{array}{l} v'(u^2-u'^2-v^2+v'^2-w^2+w'^2) + 2v(uu'-vv'-ww') \\ -w'(u^2-u'^2-2v^2+2v'^2) - 2w(uu'-2vv') \end{array} \right] \end{array} \right\}. \quad (36)$$

proportional to $[w' - vv']$ which can generate XCD *even in the case of non-gyrotropic crystals*: we may identify this term with the “*crystal optics effect*” predicted by Machavariani [7] using a different formalism. It is also noteworthy that the “*absorptive*” (w) and “*dispersive*” (w') parts of the gyrotropy tensor start to mix up in the third order term. What is however most striking in equation (30) is the decomposition into terms of *odd parity* related to gyrotropy, and terms of *even parity* which are independent of gyrotropy. One could envisage to separate experimentally the two contributions with a piezoelectric, gyrotropic crystal: let one assume that the crystal is electrically excited at some modulation frequency ω_M ; then the linear and quadratic terms could be discriminated by analyzing the dichroism response either at ω_M or $2\omega_M$. This is unfortunately unrealistic in the X-ray range.

3.2 Linear Dichroism in biaxial crystals

As already emphasized in the previous section, linear dichroism is expected to contaminate all XCD experiments performed on biaxial crystals as soon as the Poincaré component P_2 of the source is not strictly equal to zero. We want to point out here that standard XLD spectra also contain hidden information on gyrotropy. Let us first transpose equation (27) for linear dichroism:

$$\begin{aligned} [\sigma^{90^\circ} - \sigma^{0^\circ}] &= \ln \left(\frac{\varphi_{00}(z) + \phi_{01}(z)}{\varphi_{00}(z) - \phi_{01}(z)} \right) \\ &= \ln \left(1 + \frac{2\xi_{01}(z)}{1 - \xi_{01}(z)} \right) \end{aligned} \quad (31)$$

$$\begin{aligned} [\sigma^{135^\circ} - \sigma^{45^\circ}] &= \ln \left(\frac{\varphi_{00}(z) + \phi_{02}(z)}{\varphi_{00}(z) - \phi_{02}(z)} \right) \\ &= \ln \left(1 + \frac{2\xi_{02}(z)}{1 - \xi_{02}(z)} \right) \end{aligned} \quad (32)$$

where: $|\xi_{0j}| \leq 1$. To the same order of approximation as in the previous section, one obtains:

$$\begin{aligned} [\sigma^{90^\circ} - \sigma^{0^\circ}] &\approx \left\{ \begin{array}{l} 2aw'd - (ad)^2[vw + v'w'] \\ -\frac{1}{3}(ad)^3 [u'(v^2 + w'^2 + 2v'^2 + 2w^2) - u(vv' + ww')] \end{array} \right\} \end{aligned} \quad (33)$$

$$\begin{aligned} [\sigma^{135^\circ} - \sigma^{45^\circ}] &\approx \left\{ \begin{array}{l} -2av'd - (ad)^2[uw + u'w'] \\ +\frac{1}{3}(ad)^3 [v'(u^2 + w'^2 + 2u'^2 + 2w^2) - v(uu' + ww')] \end{array} \right\}. \end{aligned} \quad (34)$$

It would be erroneous to believe that Linear Dichroism is totally insensitive to crystal gyrotropy: the second order terms in equations (33, 34) are involving both w and w' . It is quite noteworthy that, exactly as in the case of XCD, the second order term involves the product of a dispersive lineshape (f) by an absorptive lineshape (g). As regards the third order term, let us observe that the terms in $\{w^2, w'^2, ww'\}$ are small in comparison with the terms of same order referring to the anisotropy of dipolar polarizability $\{u^2, u'^2, uu'\}$ or $\{v^2, v'^2, vv'\}$ so that the former can be neglected. Anyhow, no reliable information on gyrotropy can be extracted from XLD experiments unless the anisotropy in the first order polarizability is known with a very high accuracy.

3.3 Rotatory power

Optical rotation is a very weak effect in the X-ray range [18, 19], at least for uniaxial crystals. It is therefore desirable to carry out such a delicate experiment with an X-ray beam featuring a “*pure*” polarization state such as $\{P_1^0 = 1; P_2^0 = P_3^0 = 0\}$. Typically, in the experiment reported by Siddons *et al.* [20], the polarization state of the incident beam was: $P_1^0 = 1 - \varepsilon$ with ε of the order of 10^{-8} . It results from equation (17) that the optical rotation $\Delta\vartheta(z)$ is given by:

$$\Delta\vartheta(z) = \frac{1}{2} \arctan \left(\frac{\phi_{20}(z) + \phi_{21}(z)P_1^0}{\phi_{10}(z) + \phi_{11}(z)P_1^0} \right). \quad (35)$$

To the same level of approximation as before, one obtains:

see equation (36) above

The latter expression simplifies a lot in the case a uniaxial crystal with the beam propagating along the direction of the optical axis because $u = u' = v = v' = 0$:

$$\Delta\vartheta(z) \approx \frac{1}{2}aw'd. \quad (37)$$

The latter result is perfectly consistent with equation (23). Note that it is also fully consistent with a well known result of classical optics in the visible range: linear dichroism will induce a significant optical rotation in non-gyrotropic

crystals ($w = w' = 0$) as soon as the absorption is not isotropic in the plane perpendicular to the direction of propagation of the incident beam. In view of the complexity of (36), it appears practically hopeless to sort out the contribution of gyrotropy in the case of biaxial crystals and CD experiments look preferable.

3.4 Circular polarimetry

It may be tempting to analyze directly the polarization state of a transmitted beam in order to access to the individual components $S_j(d)$. With the recent availability of X-ray quarter-wave plates [21–25], circularly polarized X-ray photons can be converted with a good efficiency into linearly polarized ones with a polarization vector oriented in any desired direction: the latter component can then be selected with a linear polarimeter exploiting either coherent (*i.e.* Bragg diffraction at 45°) or incoherent scattering at 90° . As discussed elsewhere, circular polarimetry can be performed either upstream or downstream with respect to the monochromator: in the former case, one may get rid of the poor polarization transfer of the monochromator and fully exploit the high circular polarization rate of helical undulator sources [25]. As far as X-ray gyrotropy is concerned, the quantity of interest turns out to be the *inverse* of the circular asymmetry ratio denoted hereafter $\rho_3(z)$:

$$\begin{aligned} \frac{1}{\rho_3(z)} &= \frac{S_3^R(z) + S_3^L(z)}{S_3^R(z) - S_3^L(z)} \\ &= \frac{\varphi_{30}(z) + \varphi_{31}(z)P_1^0 + \varphi_{32}(z)P_2^0(1 - \varepsilon_2)}{\varphi_{33}(z)P_3^0(1 - \varepsilon_3) + \varphi_{32}(z)\varepsilon_2P_2^0} \end{aligned} \quad (38)$$

or to some degree of approximation:

$$\begin{aligned} \frac{1}{\rho_3(z)} &\approx \frac{1}{P_3^0} \xi_{30} (1 + \varepsilon_3 - \varepsilon_2 P_2^0 \xi_{32}) + \xi_{31} \frac{P_1^0}{P_3^0} \\ &\quad + \xi_{32} \frac{P_2^0}{P_3^0} (1 - \varepsilon_2). \end{aligned} \quad (39)$$

Thus, under ideal conditions ($P_1^0 = P_2^0 = 0$; $P_3^0 = 1$), one obtains:

$$\begin{aligned} \frac{1}{\rho_3(z)} &\approx \\ &\left\{ \begin{aligned} &awd - \frac{1}{2}(ad)^2[u'v - uv'] \\ &+ \frac{1}{6}(ad)^3[w(2u^2 + 2v^2 + u'^2 + v'^2) - w'(uu' + vv') - 2w^3] \end{aligned} \right\}. \end{aligned} \quad (40)$$

Up to the second order, the information content of circular polarimetry is then, within a factor 1/2, strictly equivalent to the information currently available from XCD experiments and there is no valuable additional information to be extracted from the third order term.

4 Fluorescence detected dichroism

The backscattering geometry of the experiment reported in [1] is illustrated with Figure 1. The wavevector of the

incident X-ray beam $\mathbf{k} [0, 0, 1]$ is defined with respect to the laboratory coordinate axes $\{x, y, z\}^{(1)}$ whereas the wavevector of the emitted X-ray fluorescence photons $\mathbf{k}_F [0, 0, 1]$ is defined with respect to another coordinate system $\{x', y', z'\}^{(2)}$. The two coordinate systems transform into one another by a rotation $R(\phi)$ around the normal to the scattering plane $\{\mathbf{k}, \mathbf{k}_F\}$. This is the appropriate point at which to recall that a tensor component $T_{\alpha\beta\gamma}$ will transform in rotation R as:

$$T_{\lambda\mu\nu}(x', y', z') = L_{\lambda\alpha}(R)L_{\mu\beta}(R)L_{\nu\gamma}(R)T_{\alpha\beta\gamma}(x, y, z) \quad (41)$$

where the factors $L_{\mu\beta}(R)$ are the direction cosines which specify the orientation of the new set of axes with respect to the old ones. We will use extensively equation (41) below.

4.1 Formulation of the fluorescence signal

We will restrict our analysis to the case of a spontaneous X-ray fluorescence emission associated with a radiative decay of the core hole created by the primary absorption of a polarized incident X-ray photon. Anisotropic Resonant Inelastic X-ray Scattering (RIXS) processes would require a specific theoretical framework and will be considered elsewhere. Thus, the fluorescence emitted by an ultrathin slice of crystal of thickness Δz and corresponding to a penetration depth z will be characterized by a Stokes vector $|\mathbf{S}_F\rangle$ satisfying the differential equation:

$$\begin{aligned} \frac{\partial}{\partial z} |\mathbf{S}_F(z' = 0)\rangle &= [\Gamma^F] \frac{\partial}{\partial z} |\mathbf{S}^{(1)}(z)\rangle \\ &= a [\Gamma^F] [\mathbf{M}^{(1)}] |\mathbf{S}^{(1)}(z)\rangle \end{aligned} \quad (42)$$

where, the superscripts ⁽¹⁾ or ⁽²⁾ refer to the coordinate systems $\{x, y, z\}^{(1)}$ or $\{x', y', z'\}^{(2)}$. Here $[\Gamma^F]$ is a diagonal 4×4 matrix describing the quantum yield of polarized fluorescence emission and will be defined in more detail in the next section and in Appendix A3. We need to describe the reabsorption of the *fluorescence photons* inside the crystal: this requires us to introduce *another* Müller matrix $[\Phi^{(2)}]$ so that:

$$\begin{aligned} \frac{\partial}{\partial z} |\mathbf{S}_F(z')\rangle &= \frac{1}{L_{z'z}} [\Phi^{(2)}(z')] \frac{\partial}{\partial z} |\mathbf{S}_F(z' = 0)\rangle \\ &= \frac{a}{L_{z'z}} [\Phi^{(2)}(z')] [\Gamma^F] [\mathbf{M}^{(1)}] |\mathbf{S}^{(1)}(z)\rangle \end{aligned} \quad (43)$$

or:

$$\begin{aligned} \frac{\partial}{\partial z} |S_{Fj}(z')\rangle &= \\ &= \frac{a}{L_{z'z}} \sum_{i=0}^3 \phi_{j\beta}^{(2)}(z') \Gamma_{\beta\beta}^F m_{\beta\alpha}^{(1)} \phi_{\alpha i}^{(1)}(z) [P_i^0 S_0^0]^{(1)}. \end{aligned} \quad (44)$$

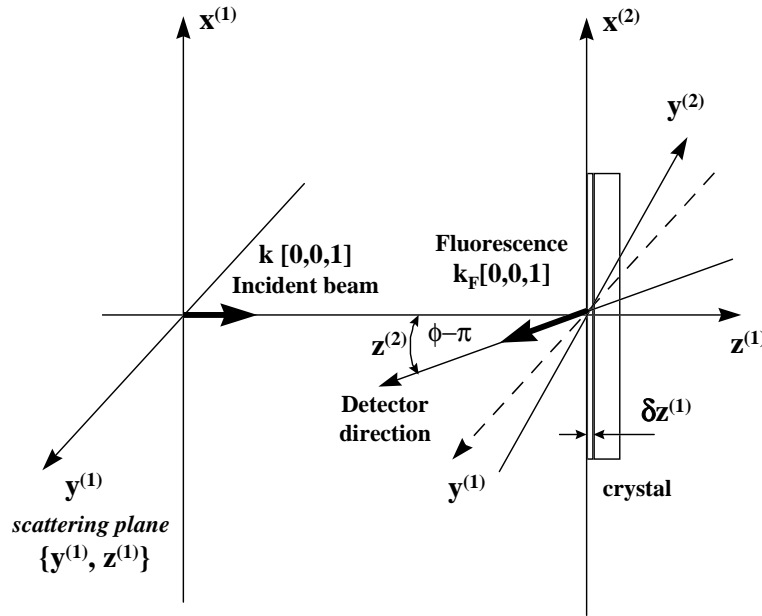


Fig. 1. Geometry for Fluorescence detected X-ray Natural Circular Dichroism (Fd-XNCD) experiments. Note that the optical axis of the crystal is colinear with the wavevector $\mathbf{k} [0, 0, 1]$ of the incident beam defined with respect to the laboratory coordinate system $\{x, y, z\}^{(1)}$, whereas the wavevector $\mathbf{k}_F [0, 0, 1]$ relative to the X-ray fluorescence photons is defined with respect to the secondary coordinate system $\{x, y, z\}^{(2)}$.

As long as the polarization of the fluorescence emission is not analyzed, only the $j = 0$ component is retained and the fluorescence signal is given by:

$$I_F = \frac{a [S_0^{01}]^{(1)}}{L_{z'z}} \int_0^d dz \sum_{i=0}^3 \phi_{0\beta}^{(2)}(z) I_{\beta\beta}^F m_{\beta\alpha}^{(1)} \phi_{\alpha i}^{(1)}(z) [P_i^{01}]^{(1)}. \quad (45)$$

The main difficulty is thus to calculate 16 integrals of the type:

$$\Psi_{\alpha\beta\gamma} = \int_0^d dz \left[\phi_{0\gamma}^{(2)}(z) \phi_{\beta\alpha}^{(1)}(z) \right]. \quad (46)$$

Fortunately, in most practical cases, the *reabsorption process can be taken as isotropic* and matrix $[\mathbf{M}^{(2)}]$ reduces to the scalar term $t'^{(2)}$ whereas $\phi_{0\gamma}^{(2)} = \delta_{0\gamma} \exp(azt'^{(2)})$: this is because a strongly anisotropic absorption can hardly be observed outside the typical energy range of X-ray Absorption Near Edge (XANES) spectra whereas the energy E_F of all *fluorescence* emission lines is systematically lower than the energy of the corresponding excitation edge. One might certainly find examples where a fluorescence line is interfering with *another* absorption edge at lower energy but such a complicated situation will not be considered here. Let us also keep in mind that isotropic reabsorption may not hold true in the case of RIXS.

4.2 Polarization of the emitted fluorescence photons

The emitted fluorescence photons may have a significant degree of polarization: this implies that $[I^F]$ is not a scalar but is a tensor property of the crystal. As shown by equation (45), we are interested here only in the four diagonal matrix elements: Γ_{jj}^F which are proportional to the four components of a *coherence vector* as defined by Born and Wolf [26,27]:

$$\Gamma_{00}^F = \gamma_0 \langle E_x^F E_x^{F*} + E_y^F E_y^{F*} \rangle = \gamma_0 \beta_F \langle -t'_F(g) \rangle^{(1)} \quad (47)$$

$$\Gamma_{11}^F = \gamma_1 \langle E_x^F E_x^{F*} - E_y^F E_y^{F*} \rangle \quad \Gamma_{11}^F = \gamma_1 \beta_F \langle -u'_F(g) \rangle^{(1)} \quad (48)$$

$$\Gamma_{22}^F = \gamma_2 \langle -[E_x^F E_y^{F*} + E_y^F E_x^{F*}] \rangle \quad \Gamma_{22}^F = -\gamma_2 \beta_F \langle -v'_F(g) \rangle^{(1)} \quad (49)$$

$$\Gamma_{33}^F = \gamma_3 \langle -i[E_x^F E_y^{F*} - E_y^F E_x^{F*}] \rangle \quad \Gamma_{33}^F = \gamma_3 \beta_F \langle w_F(g) \rangle^{(1)} \quad (50)$$

where the brackets remind us that a configuration average has to be taken over all emitting sites. Equivalently, the matrix elements Γ_{jj}^F can be expressed in terms of the absorptive components $t'_F(g)$, $u'_F(g)$, $v'_F(g)$ and $w_F(g)$ of the complex tensors $\{t_F^*, u_F^*, v_F^*, w_F^*\}$ characterizing now the emission process itself. Detailed expressions of $t'_F(g)$,

Table 1. Extended Stokes components in emission geometry without polarization analysis

Fluorescence detected XCD

$$\mathbb{S}_0^3 \approx -\frac{2I_0 P_3^0 \Gamma_{00}^F}{\cos \phi} \left\{ \begin{array}{l} w\mu + [t'w + u'v - uw']\mu^2 \\ + [t'(u'v - uw') + w(u'^2 - u^2 + v'^2 - v^2 + w^2) - w'(uu' + vv')] \mu^3 \end{array} \right\} \quad (57)$$

Fluorescence detected XLD

$$\mathbb{S}_0^1 \approx -\frac{2I_0 P_1^0 \Gamma_{00}^F}{\cos \phi} \left\{ \begin{array}{l} u'\mu + [t'u' - (vw + v'w')]\mu^2 \\ - [t'(vw + v'w') - u'(v'^2 - v^2 + u'^2 + w^2 - w'^2) - u(vv' - ww')] \mu^3 \end{array} \right\} \quad (58)$$

$$\mathbb{S}_0^2 \approx -\frac{2I_0 P_2^0 \Gamma_{00}^F}{\cos \phi} \left\{ \begin{array}{l} -v'\mu - [t'v' + uw + u'w']\mu^2 \\ - [t'(uw + u'w') + v'(u'^2 - u^2 + v'^2 + w^2 - w'^2) + v(uu' - ww')] \mu^3 \end{array} \right\}. \quad (59)$$

$u'_F(g)$, $v'_F(g)$ and $w'_F(g)$ are given in Appendix A3. Note that equation (50) would predict the existence of *X-ray gyrotropic emission* in addition to *X-ray gyrotropic absorption*. Such a gyrotropic emission is still unknown in the X-ray range: it would be the X-ray analog of the so-called *Circularly Polarized Luminescence* (CPL) which is a well established chiroptical spectroscopy in the visible range [28–30]. Unfortunately, the only terms which might contribute to a gyrotropic emission in the X-ray range are again electric dipole–electric quadrupole interference terms ($E_1.E_2$) which vanish in powder or solutions. Moreover, since the ($E_1.E_2$) interference terms probe the overlap in energy of states of different parity [3], there is very little or no hope to detect any gyrotropic emission for fluorescence lines involving only transitions between deep atomic core levels (*e.g.* the K_α lines). Gyrotropic emission could then be detectable only in very few cases: (*i*) for fluorescence lines associated with transitions in which a deep core hole is filled by valence electrons; (*ii*) for RIXS processes which fall out of the scope of the present paper. Let us recall that a quite significant degree of circular polarization has already been measured in *X-ray Excited Optical Luminescence* (XEOL) spectra [31].

4.3 Fluorescence detected dichroism spectra

In this section, we will concentrate first on fluorescence detected dichroism spectra recorded *without polarization analysis* because such experiments have already been performed. For the sake of clarity, it is most convenient to define “*extended*” Stokes components $\mathbb{S}_{F(j)}^{I(i)}$ with two indices: the lower index would characterize the emitted fluorescence beam and the upper one would refer to the incident beam. As long as we do not analyze the polarization states of the emitted photons, we are concerned only with

the three components:

$$\mathbb{S}_0^1 = S_{F(0)}^{I(90^\circ)} - S_{F(0)}^{I(0^\circ)} \quad (51)$$

$$\mathbb{S}_0^2 = S_{F(0)}^{I(135^\circ)} - S_{F(0)}^{I(45^\circ)} \quad (52)$$

$$\mathbb{S}_0^3 = S_{F(0)}^{I(L)} - S_{F(0)}^{I(R)}. \quad (53)$$

For infinitely thick samples, one would show that:

$$\mathbb{S}_0^i = -\frac{2aI_0 P_i^0 \Gamma_{00}^F}{L_{z'z}} \int_0^\infty dz \exp(-az/\mu) [\mathbf{M}\Phi]_{0i} \quad (54)$$

where we have introduced the simplifying notation: $1/\mu = -[t'^{(1)} + t'^{(2)}]$. Combining the following identities:

$$\int_0^\infty dz \exp(-az/\mu) \cos(az\lambda) = \frac{\mu}{a(1 + \lambda^2\mu^2)} \quad (55)$$

$$\int_0^\infty dz \exp(-az/\mu) \sin(az\lambda) = \frac{\lambda\mu^2}{a(1 + \lambda^2\mu^2)} \quad (56)$$

with the series expansion of $[\Phi(z)]$ developed in Appendix A2, one is led to the final results listed in Table 1 (Eqs. (57–59)).

By comparing equation (57) with equation (30), it will immediately appear that Fd-CD is strictly proportional to transmission circular dichroism in the case of uniaxial crystals when the incident beam propagates along the direction of the optical axis. In the case of biaxial crystals, this proportionality still holds true for the first order term with respect to μ . Regarding the second and third order terms, it appears again that non-gyrotropic crystals with $w = w' = 0$ should exhibit non-zero Fd-XCD spectra if $(u'v - v'u) \neq 0$: this was precisely the condition discussed

earlier in Section 3 to observe the so-called “*crystal optics effect*” of Machavariani [7]. It is however quite remarkable that in the case of gyrotropic crystals, the leading second order term of \mathbb{S}_0^3 should be $wt'\mu^2$ (which is proportional to the isotropic absorption t') rather than $(u'v - v'u)\mu^2$. This additional term $wt'\mu^2$ does not exist in transmission CD experiments but it makes the analyses far more comfortable if one is interested in sorting out clean gyrotropy spectra: in other terms, Fd-XCD offers the significant advantage over XCD to depress the relative contribution of the unwanted “crystal optics effects”. Of course, one could draw symmetrical conclusions if one compares the analytical expressions derived for Fd-XLD and transmission linear dichroism experiments.

The previous discussion concerned “*ideal experimental conditions*”, *e.g.* $P_1^0 = P_2^0 = 0$; $P_3^0 = \pm 1$. Indeed, Fd-XCD spectra of biaxial crystals are, under real experimental conditions, also systematically contaminated by unwanted linear dichroism signatures:

$$[\mathbb{S}_0^3]_{\text{apparent}} = (1 - \varepsilon_3/2)\mathbb{S}_0^3 + \varepsilon_2\mathbb{S}_0^2. \quad (60)$$

4.4 Polarization analysis of emission spectra

We may investigate next whether new information could be extracted from a careful analysis of the polarization state of the fluorescence photons. The following integrals have now to be calculated:

$$\mathbb{S}_j^i = -\frac{2aI_0P_i^0\Gamma_{jj}^F}{L_{z'z}} \int_0^\infty dz \exp(-az/\mu) [\mathbf{M}\Phi]_{ji} \quad (61)$$

and, to the same level of approximation as before, one would derive the following results:

4.4.1 Incident X-ray beam circularly polarized

$$\mathbb{S}_1^3 \approx -\frac{2I_0P_3^0\Gamma_{11}^F}{\cos\phi} \{v\mu + [t'v + u'w - uw']\mu^2\} \quad (62)$$

$$\mathbb{S}_2^3 \approx -\frac{2I_0P_3^0\Gamma_{22}^F}{\cos\phi} \{u\mu + [t'u - v'w + vw']\mu^2\} \quad (63)$$

$$\mathbb{S}_3^3 \approx -\frac{2I_0P_3^0\Gamma_{33}^F}{\cos\phi} \{t'\mu - [u^2 + v^2 - w^2]\mu^2\}. \quad (64)$$

4.4.2 Incident X-ray beam linearly polarized ($90^\circ - 0^\circ$)

$$\mathbb{S}_1^1 \approx -\frac{2I_0P_1^0\Gamma_{11}^F}{\cos\phi} \{t'\mu + [u^2 - v^2 - w^2]\mu^2\} \quad (65)$$

$$\mathbb{S}_2^1 \approx -\frac{2I_0P_1^0\Gamma_{22}^F}{\cos\phi} \{w'\mu + [t'w' - u'v' - uv]\mu^2\} \quad (66)$$

$$\mathbb{S}_3^1 \approx -\frac{2I_0P_1^0\Gamma_{33}^F}{\cos\phi} \{-v\mu - [t'v - u'w + uw']\mu^2\}. \quad (67)$$

Table 2. Electric polarizability tensors contributing to the first order in μ in the absorption and emission processes. Let us recall that t', u', v' and w refer to absorptive parts and u, v and w' to dispersive parts. Do not confuse $t^{(2)}$ and t'_F which refer to different matrix elements: the former is describing the reabsorption of the fluorescence photons at energy E_F whereas the latter describes the spontaneous emission process.

$\mathbf{j}\mathbf{i}$	$i = 1$	$i = 2$	$i = 3$	Γ_{jj}^F
$j = 0$	u'	$-v'$	w	$-t'_F$
$j = 1$	t'	w'	$-v$	$-u'_F$
$j = 2$	$-w'$	t'	$-u$	$-v'_F$
$j = 3$	v	u	t'	w_F

4.4.3 Incident X-ray beam linearly polarized ($135^\circ - 45^\circ$)

$$\mathbb{S}_1^2 \approx -\frac{2I_0P_2^0\Gamma_{11}^F}{\cos\phi} \{-w'\mu - [t'w' + u'v' + uv]\mu^2\} \quad (68)$$

$$\mathbb{S}_2^2 \approx -\frac{2I_0P_2^0\Gamma_{22}^F}{\cos\phi} \{t'\mu + [v'^2 - u^2 - w'^2]\mu^2\} \quad (69)$$

$$\mathbb{S}_3^2 \approx -\frac{2I_0P_2^0\Gamma_{33}^F}{\cos\phi} \{-u\mu - [t'u + v'w - vw']\mu^2\}. \quad (70)$$

Indeed, the 12 extended Stokes components \mathbb{S}_j^i listed above will again simplify a lot in the case of uniaxial crystals since only the first order terms with respect to μ will survive. We have regrouped in Table 2 the polarizability tensors contributing to the first order terms for the various combinations of indices i and j .

Note that in the case of uniaxial crystals, $u = u' = 0$ and $v = v' = 0$ for what concerns the primary absorption process but $\Gamma_{11}^F \neq 0$, $\Gamma_{22}^F \neq 0$ since, in a gyrotropic crystal, the components of the polarizability tensor are different in directions respectively parallel or perpendicular to the optical axis. One could use a linearly polarized incident beam (selecting for instance: $i = 2$) and analyze the relevant linearly polarized components of the emitted photons (*e.g.* $j = 1$ if $i = 2$): this experiment should give access to $w'(f)$, *i.e.* the *dispersive* part of the gyrotropy tensor. The information available from the latter experiment is then strictly equivalent to what can be learned from *optical rotation measurements in transmission*. A considerable advantage of such “*Fluorescence detected X-ray Optical Rotation*” (Fd-XOR) experiments is indeed the possibility to exploit this technique even *with thick crystals* for which conventional XOR measurements are impossible. Actually, what would be measured in Fd-XOR is not $w'(f)$ but the product $\Gamma_{11}^F w'(f)$ which may also depend on the anisotropy of the emission process. One could circumvent the latter complication by performing the same polarization analysis with both $i = 1$ and $i = 2$ since the ratio: $[\mathbb{S}_1^2/\mathbb{S}_1^1] \simeq w'(f)/t'(g)$ would be independent of the anisotropy of the emission process.

Even though the case of biaxial crystals looks inherently far more complicated, it might still be attractive to try to measure the three components \mathbb{S}_j^i . The last

one, (*i.e.* $i = 3$) would give us a unique, unambiguous access to gyrotropy in the emission channel. On the other hand, one might envisage to disentangle the contribution of the so-called “*crystal optics effect*” because: $[\mathbb{S}_3^1 \mathbb{S}_0^1 + \mathbb{S}_3^2 \mathbb{S}_0^2] / \mathbb{S}_3^3 \simeq -[u'v - v'u] \Gamma_{00}^F / t'$. Unfortunately, at the present stage of the technique, X-ray fluorescence emission with polarization analysis looks like an experimental *tour de force*, especially in terms of signal-to-noise ratio, and it remains to be proved that one can really measure this second order contribution.

5 Discussion

It is well known from general quantum mechanics that absorption processes are truly measurable only if they are associated with anti-hermitian, time-even tensor properties. Since this condition has to be satisfied by all tensor properties contributing to linear or circular dichroism, we feel essential to cross-check the consistency of our results.

5.1 Antisymmetric character of dichroism tensors

As illustrated by equation (30), the tensor property responsible for circular dichroism is to the first order $w(g)$ which, according to equation (12), is the sum of 3 antisymmetric tensors. One may easily establish the antisymmetric character of all higher order terms: typically the quantity $[u(g)v'(f) - v(g)u'(f)]$ will change its sign on exchanging x and y because this term is, by definition, the cross product of symmetric tensors $\{v, v'\}$ by antisymmetric ones $\{u, u'\}$. The same sort of consideration can be extended to the various terms contributing to linear dichroism: *e.g.* $\{u, u'\}$ reverse their sign on exchanging x and y and are thus antisymmetric. On the contrary, $\{v, v'\}$ which are symmetrical tensors cannot contribute to any measurable linear dichroism unless the polarization vector is rotated by $\pm 45^\circ$ so that the roles of $\{u, u'\}$ and $\{v, v'\}$ are finally exchanged.

5.2 Rotational invariance of circular dichroism around the incident beam direction

This is a well known property and a common argument used to reject possible instrumental artifacts. Using equation (41), it is straightforward to show that $w(g)$, $w'(f)$ and $[u(g)v'(f) - v(g)u'(f)]$ are invariant in any rotation around the direction of the wavevector \mathbf{k} . Thus, there is absolutely no hope to discriminate between $w(g)$ and $[u(g)v'(f) - v(g)u'(f)]$ by simply rotating the crystal around the direction of the incident beam. This result is indeed comforting our interpretation that the cross term $[u(g)v'(f) - v(g)u'(f)]$ is to be identified with the dispersion term derived by Born and Huang in a dielectric crystal [32]: as pointed out only very recently by Nelson [33], this second order term was the only one found by Born and Huang because they neglected in their theory the interaction of electric dipoles with either magnetic dipoles or electric quadrupoles.

5.3 Time-reversality

As emphasized by Barron [4] and others [35,36], the tensors $\{\alpha_{\alpha\beta}; \zeta'_{\alpha\beta\gamma}; Q_{\alpha\gamma\beta}\}$ have *time even parity* with respect to the action of the time-reversal operator: $\{\alpha_{\alpha\beta}; Q_{\alpha\gamma\beta}\}$ are then responsible for *natural* linear dichroism whereas $\{\zeta'_{\alpha\beta\gamma}\}$ contributing to w is responsible for *natural* circular dichroism. In contrast, $\{\alpha'_{\alpha\beta}; \zeta_{\alpha\beta\gamma}; Q'_{\alpha\gamma\beta}\}$ have *time odd parity* with respect to the action of the time-reversal operator and cannot contribute to any dichroism unless another time-odd perturbation is present: this may be the case of an external magnetic field or of an internal exchange field. In other words, $\{\alpha'_{\alpha\beta}; \zeta_{\alpha\beta\gamma}; Q'_{\alpha\gamma\beta}\}$ will induce magnetic linear (or magnetic circular) dichroisms provided that there is a magnetic field oriented along the direction of propagation of the incident beam. It is precisely well documented that $\alpha'_{\alpha\beta}$ and $Q'_{\alpha\gamma\beta}$ are contributing to X-ray magnetic circular dichroism. It has also been suggested a long time ago by Brown *et al.* [34] and by other groups [4,35,36] that the symmetrical part of the gyrotropy tensor $\zeta_{\alpha\beta\gamma}$ could be responsible for “*non-reciprocal*” birefringence in antiferromagnetic crystals which have a non-zero magnetoelectric tensor. The reality of this effect was confirmed only quite recently at optical wavelengths [37]. Since $\zeta_{\alpha\beta\gamma}$ contributes to the definition of the anisotropy tensor u' in equation (9), our analysis would predict that the “*non-reciprocal*” gyrotropy should generate a *non-reciprocal X-ray magnetic linear dichroism*. Even though the “*non-reciprocal*” gyrotropy tensor cannot contribute to any first order X-ray circular dichroism, we think that circular dichroism could still arise through the second order cross term $[uv' - vu']$ which combines products of the type: $\zeta_{xyz}(f)\alpha_{xx}(g)$; $\zeta_{xyz}(f)\alpha_{yy}(g)$; $\zeta_{xxz}(g)\alpha_{xy}(f)$; $\zeta_{yyz}(g)\alpha_{xy}(f)$; $\zeta_{xyz}(g)\alpha_{xx}(f)$; $\zeta_{xyz}(g)\alpha_{yy}(f)$; $\zeta_{xxz}(f)\alpha_{xy}(g)$; $\zeta_{yyz}(f)\alpha_{xy}(g)$ and in which the dipolar contribution associated with $\alpha_{\alpha\beta}(g)$ may be large.

6 Conclusion

For the first time, we have proposed a unified formulation of the differential absorption and differential change of polarization state of a polarized X-ray beam propagating inside a biaxial gyrotropic crystal. The starting point of this analysis is a 4×4 differential Müller matrix, the 16 elements of which are related to the anisotropic components of the multipolar polarizability tensors at the absorbing site. Our primary goal was to derive analytical expressions for X-ray linear and circular dichroism, optical rotation and circular polarimetry in a transmission configuration. The same formalism has been extended to encompass the case of Fluorescence detected X-ray dichroism, which is a technique of much more practical interest. Analytical expressions have been obtained for the “*extended*” Stokes components \mathbb{S}_j^i of the emitted photons: our results confirm that more information could be obtained if one could analyze –*at least*– the linear polarization components of the X-ray fluorescence emitted in a specific direction.

In the case of biaxial crystals, we face serious problems since the tiny effects of X-ray gyrotropy in circular dichroism may be completely swamped out by large linear dichroism signals mostly due to the imperfect polarization transfer of X-ray monochromators. It is shown that Fd-XCD spectra are not anymore strictly proportional to transmission XCD spectra. As far as circular dichroism is concerned, one has also to take into account a possible contribution of second order terms: even in the case of non-gyrotropic crystals, one should record non-zero XCD spectra whenever the condition: $[u(g)v'(f) - v(g)u'(f)] \neq 0$ is satisfied. Since this contribution is also invariant in any rotation around the direction of the incident beam, it appears *a priori* fairly difficult to discriminate normal gyrotropy effects from the latter “*crystal optics effect*” the existence of which was predicted by Machavariani [7]. Interestingly, the relative importance of this contribution has been found to be depressed in Fd-XCD spectra.

Last but not least, we checked the consistency of our results with respect to antisymmetry and time reversal properties. Our formulation of linear and circular dichroism in gyrotropic crystals includes terms of odd parity with respect to the action of the time reversal operator: the terms responsible for X-ray magnetic circular dichroism in anisotropic crystals are well identified but we obtain additional terms which cannot contribute to any natural X-ray linear nor circular dichroism but may well cause *non-reciprocal* X-ray gyrotropy effects in antiferromagnetic crystals.

Appendix A1

Following Buckingham [10], one may define at the absorbing site a variety of multipolar polarizability tensor components:

$$\begin{aligned} \alpha_{\alpha\beta}(f^*) &= +\alpha_{\beta\alpha}(f^*) \\ &= \frac{2}{\hbar} \sum_j f^* \omega_{ij}^* \operatorname{Re} \{ \langle i | E_{1\alpha} | j \rangle \langle j | E_{1\beta} | i \rangle \} \quad (71) \end{aligned}$$

$$\begin{aligned} \alpha'_{\alpha\beta}(f^*) &= -\alpha'_{\beta\alpha}(f^*) \\ &= -\frac{2}{\hbar} \sum_j f^* \omega \operatorname{Im} \{ \langle i | E_{1\alpha} | j \rangle \langle j | E_{1\beta} | i \rangle \} \quad (72) \end{aligned}$$

$$\begin{aligned} A_{\alpha\beta\gamma}(f^*) &= +A_{\alpha\gamma\beta}(f^*) \\ &= \frac{2}{\hbar} \sum_j f^* \omega_{ij}^* \operatorname{Re} \{ \langle i | E_{1\alpha} | j \rangle \langle j | E_{2\beta\gamma} | i \rangle \} \quad (73) \end{aligned}$$

$$\begin{aligned} A'_{\alpha\beta\gamma}(f^*) &= +A'_{\alpha\gamma\beta}(f^*) \\ &= -\frac{2}{\hbar} \sum_j f^* \omega \operatorname{Im} \{ \langle i | E_{1\alpha} | j \rangle \langle j | E_{2\beta\gamma} | i \rangle \} \quad (74) \end{aligned}$$

$$G_{\alpha\beta}(f^*) = \frac{2}{\hbar} \sum_j f^* \omega_{ij}^* \operatorname{Re} \{ \langle i | E_{1\alpha} | j \rangle \langle j | M_{1\beta} | i \rangle \} \quad (75)$$

$$G'_{\alpha\beta}(f^*) = -\frac{2}{\hbar} \sum_j f^* \omega \operatorname{Im} \{ \langle i | E_{1\alpha} | j \rangle \langle j | M_{1\beta} | i \rangle \} \quad (76)$$

$$\begin{aligned} C_{\alpha\beta\gamma\delta}(f^*) &= +C_{\gamma\delta\alpha\beta}(f^*) \\ &= \frac{2}{3\hbar} \sum_j f^* \omega_{ij}^* \operatorname{Re} \{ \langle i | E_{2\alpha\beta} | j \rangle \langle j | E_{2\gamma\delta} | i \rangle \} \quad (77) \end{aligned}$$

$$\begin{aligned} C'_{\alpha\beta\gamma\delta}(f^*) &= -C'_{\gamma\delta\alpha\beta}(f^*) \\ &= \frac{2}{3\hbar} \sum_j f^* \omega \operatorname{Im} \{ \langle i | E_{2\alpha\beta} | j \rangle \langle j | E_{2\gamma\delta} | i \rangle \} \quad (78) \end{aligned}$$

where E_1 , M_1 and E_2 refer to the electric dipole, magnetic dipole and electric quadrupole operators. In the case of mixed multipole components (73, 74; 75, 76), there is no direct separation into symmetric / antisymmetric parts with respect to the exchange of the first two indices and it is therefore much convenient to generate two additional tensors which are *symmetric* or *antisymmetric* with respect to the exchange of these indices:

$$\begin{aligned} \zeta_{\alpha\beta\gamma} &= +\zeta_{\beta\alpha\gamma} \\ &= +\frac{1}{c} \left\{ \frac{\omega}{3} [A'_{\alpha\beta\gamma} + A'_{\beta\alpha\gamma}] + \epsilon_{\delta\gamma\alpha} G_{\beta\delta} + \epsilon_{\delta\gamma\beta} G_{\alpha\delta} \right\} \quad (79) \end{aligned}$$

$$\begin{aligned} \zeta'_{\alpha\beta\gamma} &= -\zeta'_{\beta\alpha\gamma} \\ &= -\frac{1}{c} \left\{ \frac{\omega}{3} [A_{\alpha\beta\gamma} - A_{\beta\alpha\gamma}] + \epsilon_{\delta\gamma\alpha} G'_{\beta\delta} - \epsilon_{\delta\gamma\beta} G'_{\alpha\delta} \right\} \quad (80) \end{aligned}$$

where c is the velocity of light and $\epsilon_{\alpha\beta\gamma}$ is the Levi-Civita alternating tensor. The tensor (80) is to be identified with a microscopic gyrotropy tensor whereas the tensor (79) may be called “*non-reciprocal gyrotropy tensor*” for reasons which are discussed in Section 5. In equations (71–80), the complex function f^* is defined by:

$$\begin{aligned} f^* &= f + ig \\ &= \frac{(\omega_{ij})^2 - \omega^2}{[(\omega_{ij})^2 - \omega^2]^2 + [\omega\Gamma_j]^2} + i \frac{\omega\Gamma_j}{[(\omega_{ij})^2 - \omega^2]^2 + [\omega\Gamma_j]^2} \quad (81) \end{aligned}$$

where f and g are the well known dispersive and absorptive lineshapes. One may also define the complex transition energy: $\omega_{ij}^* = \omega_{ij} - i\Gamma_j/2$, where Γ_j is the full width at half maximum (fwhm) of a Lorentzian lineshape and, as far as X-ray absorption spectroscopy is concerned, the latter parameter refers to the life time of the deep core hole in the excited state. As discussed elsewhere [1, 5], the magnetic dipole (M_1) transition matrix elements (TME) are expected to be very small in the X-ray range but we decided to maintain the terms (75, 76) for the sake of completeness of the final results which may then be more easily extrapolated into other energy ranges. On the other hand, there is ample experimental evidence [5, 11–15] that X-ray absorption spectroscopy is sensitive to the pure electric quadrupole ($E_2.E_2$) cross sections: this implies that the terms (77, 78) cannot be neglected in the X-ray range.

In the theory of refringent scattering developed by Buckingham [10] or Barron [4], it is finally most convenient to introduce the following *complex* multipolar

polarizability tensors $\alpha_{\alpha\beta}^*$, $C_{\alpha\beta\gamma\delta}^*$ and $\zeta_{\alpha\beta\gamma}^*$ respectively defined as:

$$\alpha_{\alpha\beta}^* = \left[\alpha_{\alpha\beta}(f) + \alpha'_{\alpha\beta}(g) \right] + i \left[\alpha_{\alpha\beta}(g) - \alpha'_{\alpha\beta}(f) \right] \quad (82)$$

$$C_{\alpha\beta\gamma\delta}^* = \left[C_{\alpha\beta\gamma\delta}(f) + C'_{\alpha\beta\gamma\delta}(g) \right] + i \left[C_{\alpha\beta\gamma\delta}(g) - C'_{\alpha\beta\gamma\delta}(f) \right] \quad (83)$$

$$\zeta_{\alpha\beta\gamma}^* = \left[\zeta_{\alpha\beta\gamma}(f) + \zeta'_{\alpha\beta\gamma}(g) \right] + i \left[\zeta_{\alpha\beta\gamma}(g) - \zeta'_{\alpha\beta\gamma}(f) \right]. \quad (84)$$

For the sake of simplifying the notations, it was found preferable to replace $C_{\alpha\gamma\gamma\beta}^*$ in equation (1) with:

$$Q_{\alpha\gamma\gamma\beta}^* = \frac{(\omega)^2}{3c^2} C_{\alpha\gamma\gamma\beta}^*.$$

Appendix A2

Let us define the matrix $[\mathbf{M}']$, which is the differential Müller matrix $[\mathbf{M}]$ of equation (15) but *without the diagonal elements*, and its associated matrix $[\mathbf{M}'']$ such as:

$$[\mathbf{M}'] = \begin{bmatrix} 0 & u' & -v' & w' \\ u' & 0 & -w' & v \\ -v' & w' & 0 & u \\ w' & -v' & -u' & 0 \end{bmatrix} \quad [\mathbf{M}''] = \begin{bmatrix} 0 & -u & v & w' \\ -u & 0 & w & v' \\ v & -w & 0 & u' \\ w' & -v' & -u' & 0 \end{bmatrix}. \quad (85)$$

We may next define two conjugated complex matrices such as: $[\mathbf{M}^+] = [\mathbf{M}'] + i[\mathbf{M}'']$ and $[\mathbf{M}^-] = [\mathbf{M}'] - i[\mathbf{M}'']$. It is then easy to check that the latter two matrices have the remarkable properties:

$$[\mathbf{M}^+]^2 = -\Delta^2 [\mathbf{I}_d] \quad [\mathbf{M}^-]^2 = -\Delta^{*2} [\mathbf{I}_d] \quad (86)$$

where: $\Delta^2 = (u+iu')^2 + (v+iv')^2 - (w+iw')^2$ and where Δ^* is the complex conjugate of Δ . Therefore, any exponential matrix of $\lambda[\mathbf{M}^\pm]$ can be decomposed as the sum of a term proportional to the identity matrix $[\mathbf{I}_d]$, plus a term proportional to $[\mathbf{M}^\pm]$. More precisely, we have:

$$\exp(\lambda[\mathbf{M}^+]) = \cos(\lambda\Delta) [\mathbf{I}_d] + \frac{1}{\Delta} \sin(\lambda\Delta) [\mathbf{M}^+] \quad (87)$$

$$\exp(\lambda[\mathbf{M}^-]) = \cos(\lambda\Delta^*) [\mathbf{I}_d] + \frac{1}{\Delta^*} \sin(\lambda\Delta^*) [\mathbf{M}^-] \quad (88)$$

Since $[\mathbf{M}^+]$ and $[\mathbf{M}^-]$ commute, it is straightforward to show that a more convenient analytical formulation of the integrated Müller matrix $[\Phi'](z) = \exp(az[\mathbf{M}']) = \exp(\frac{1}{2}az[\mathbf{M}^+ + \mathbf{M}^-])$ is:

$$[\Phi'](z) = \left\{ \cos(az\Delta/2) [\mathbf{I}_d] + \frac{1}{\Delta} \sin(az\Delta/2) [\mathbf{M}^+] \right\} \times \left\{ \cos(az\Delta^*/2) [\mathbf{I}_d] + \frac{1}{\Delta^*} \sin(az\Delta^*/2) [\mathbf{M}^-] \right\}. \quad (89)$$

Indeed, the diagonal element of $[\mathbf{M}]$ can be reintroduced in the final result by simply multiplying $[\Phi'](z)$ by the exponential factor $\exp(azt')$:

$$[\Phi(z)] = \exp(azt') [\Phi'(z)]. \quad (90)$$

The analytical formula derived in this paper are then based on the fairly usual series expansions of the com-

plex functions: $\cos(az\Delta/2)$; $\cos(az\Delta^*/2)$; $\sin(az\Delta/2)$ and $\sin(az\Delta^*/2)$.

Appendix A3

Our goal in this appendix is to make explicit the matrix elements Γ_{jj}^F . Starting with the definition of the *coherence vector* by Born and Wolf [26,27], the four diagonal matrix elements can be expressed in the crystal coordinate system as:

$$\Gamma_{00}^F = \gamma_0 \left\langle [E_x^F E_x^{F*} + E_y^F E_y^{F*}] - [E_y^F E_y^{F*} - E_z^F E_z^{F*}] \sin^2 \phi + [E_y^F E_z^{F*} + E_z^F E_y^{F*}] \sin \phi \cos \phi \right\rangle \quad (91)$$

$$\Gamma_{11}^F = \gamma_1 \left\langle [E_x^F E_x^{F*} - E_y^F E_y^{F*}] + [E_y^F E_y^{F*} - E_z^F E_z^{F*}] \sin^2 \phi + [E_y^F E_z^{F*} - E_z^F E_y^{F*}] \sin \phi \cos \phi \right\rangle \quad (92)$$

$$\Gamma_{22}^F = \gamma_2 \left\langle -[E_x^F E_y^{F*} + E_y^F E_x^{F*}] \cos \phi - [E_x^F E_z^{F*} + E_z^F E_x^{F*}] \sin \phi \right\rangle \quad (93)$$

$$\Gamma_{33}^F = \gamma_3 \left\langle -i [E_x^F E_y^{F*} - E_y^F E_x^{F*}] \cos \phi - i [E_x^F E_z^{F*} - E_z^F E_x^{F*}] \sin \phi \right\rangle \quad (94)$$

where the scalar factors γ_i ($\delta\Omega/4\pi$) are the quantum yields of anisotropic fluorescence in a solid angle $\delta\Omega/4\pi$. The latter solid angle is defined either by the angular acceptance of the detector or by the acceptance of the crystal analyzer when energy resolved emission spectra are recorded. Since the *coherent* fluorescence intensities $\langle E_\alpha^F E_\beta^{F*} \rangle$ are proportional to the anisotropic transition probabilities, one may write:

$$\Gamma_{00}^F = \gamma_0 \beta_F \langle -t'_F(g) \rangle^{(1)} \quad (95)$$

$$\Gamma_{11}^F = \gamma_1 \beta_F \langle -u'_F(g) \rangle^{(1)} \quad (96)$$

$$\Gamma_{22}^F = -\gamma_2 \beta_F \langle -v'_F(g) \rangle^{(1)} \quad (97)$$

$$\Gamma_{33}^F = \gamma_3 \beta_F \langle w_F(g) \rangle^{(1)} \quad (98)$$

where $\beta_F \propto \omega_F^2$ is a conversion factor which is proportional to the square of the fluorescence energy. By analogy with equations (7-13), one may then write:

$$-t'_F = \left\langle \begin{aligned} & [\alpha_{xx}^F + \alpha_{yy}^F] - [\alpha_{yy}^F - \alpha_{zz}^F] \sin^2 \phi + [\alpha_{yz}^F + \alpha_{zy}^F] \sin \phi \cos \phi \\ & + [\zeta_{xxz}^F + \zeta_{yyz}^F] n_z \cos^2 \phi - [\zeta_{yyz}^F - \zeta_{zzz}^F] n_z \cos^2 \phi \sin^2 \phi \\ & + [\zeta_{xxy}^F + \zeta_{yyy}^F] n_y \sin^2 \phi - [\zeta_{yyy}^F - \zeta_{zzz}^F] n_y \sin^4 \phi \\ & + 2[\zeta_{yzz}^F \sin \phi \cos \phi] n_z \cos^2 \phi + 2[\zeta_{yzy}^F \sin \phi \cos \phi] n_y \sin^2 \phi \end{aligned} \right\rangle \quad (99)$$

$$-u'_F = \left\langle \begin{aligned} & [\alpha_{xx}^F - \alpha_{yy}^F] + [\alpha_{yy}^F - \alpha_{zz}^F] \sin^2 \phi - [\alpha_{yz}^F + \alpha_{zy}^F] \sin \phi \cos \phi \\ & + [\zeta_{xxz}^F - \zeta_{yyz}^F] n_z \cos^2 \phi + [\zeta_{yyz}^F - \zeta_{zzz}^F] n_z \cos^2 \phi \sin^2 \phi \\ & + [\zeta_{xxy}^F - \zeta_{yyy}^F] n_y \sin^2 \phi + [\zeta_{yyy}^F - \zeta_{zzz}^F] n_y \sin^4 \phi \\ & - 2[\zeta_{yzz}^F \sin \phi \cos \phi] n_z \cos^2 \phi - 2[\zeta_{yzy}^F \sin \phi \cos \phi] n_y \sin^2 \phi \end{aligned} \right\rangle \quad (100)$$

$$-v'_F = \left\langle \begin{array}{l} 2\alpha_{xy}^F \cos \phi + 2\alpha_{xz}^F \sin \phi \\ +2 [\zeta_{xyz}^F \cos \phi + \zeta_{zzz}^F \sin \phi] n_z \cos^2 \phi \\ +2 [\zeta_{xyy}^F \cos \phi + \zeta_{xzy}^F \sin \phi] n_y \sin^2 \phi \end{array} \right\rangle \quad (101)$$

$$w_F = \left\langle \begin{array}{l} 2\alpha'_{xy} \cos \phi + 2\alpha'_{xz} \sin \phi \\ +2 [\zeta'_{xyz} \cos \phi + \zeta'_{zzz} \sin \phi] n_z \cos^2 \phi \\ +2 [\zeta'_{xyy} \cos \phi + \zeta'_{xzy} \sin \phi] n_y \sin^2 \phi \end{array} \right\rangle. \quad (102)$$

For simplicity, the “pure” electric quadrupole ($E_2.E_2$) transition matrix elements have been deliberately omitted in the latter equations. The brackets imply that one has to take a configuration average over all emitting atoms: anisotropic emission can thus only be observed in oriented single crystals but certainly not in powders nor in solution.

References

1. J. Goulon, C. Goulon-Ginet, A. Rogalev, V. Gotte, C. Malgrange, Ch. Brouder, C.R. Natoli, *J. Chem. Phys.* **108**, 6394 (1998).
2. L. Alagna, T. Proserpi, S. Turchini, J. Goulon, A. Rogalev, C. Goulon-Ginet, C.R. Natoli, B. Stewart, R.D. Peacock, *Phys. Rev. Lett.* **80**, 4799 (1998).
3. C.R. Natoli, Ch. Brouder, Ph. Sainctavit, J. Goulon, C. Goulon-Ginet, A. Rogalev, *Eur. Phys. J. B* **4**, 1 (1998).
4. L.D. Barron, *Molecular Light Scattering and Optical Activity* (Cambridge University Press, 1982).
5. Ch. Brouder, *J. Phys.-Cond. Matter* **2**, 701 (1990).
6. T. Lippmann, A. Kirfel, K. Fischer, *J. Appl. Cryst.* **29**, 186 (1996).
7. V.Sh. Machavariani, *J. Phys.-Cond. Matter* **7**, 5151 (1995).
8. L.D. Barron, A.D. Buckingham, *Mol. Phys.* **20**, 1111 (1971).
9. A.D. Buckingham, R.E. Raab, *Proc. R. Soc. London A* **345**, 365 (1975).
10. A.D. Buckingham, *Adv. Chem. Phys.* **12**, 107 (1968).
11. J.E. Penner-Hahn, R.A. Scott, K.O. Hodgson, S. Doniach, S.R. Desjardins, E.I. Solomon, *Chem. Phys. Lett.* **88**, 595 (1982).
12. G. Dräger, R. Frahm, G. Materlick, O. Brümmer, *Phys. Stat. Sol. B* **146**, 287 (1988).
13. J.C. Lang, G. Strajer, C. Detlefs, A.I. Goldman, H. König, Xindong Wang, B.N. Harmon, R.W. McCallum, *Phys. Rev. Lett.* **74**, 4935 (1995).
14. C. Giorgetti, E. Dartyge, Ch. Brouder, F. Baudelet, C. Meyer, S. Pizzini, A. Fontaine, R.M. Galera, *Phys. Rev. Lett.* **75**, 3186 (1995).
15. M.H. Krisch, C.C. Kao, F. Sette, W.A. Caliebe, K. Hämäläinen, J. Hastings, *Phys. Rev. Lett.* **74**, 4931 (1995).
16. P. Elleaume, *J. Synchrotron Rad.* **1**, 19 (1994).
17. C. Malgrange, C. Carvahlo, L. Braicovich, J. Goulon, *Nucl. Instrum. Methods A* **308**, 390 (1991).
18. M. Hart, *Philos. Mag. B* **38**, 41 (1978).
19. M. Sauvage, C. Malgrange, J.F. Petroff, *J. Appl. Cryst.* **16**, 14 (1983).
20. D.P. Siddons, M. Hart, Y. Amemiya, J.B. Hastings, *Phys. Rev. Lett.* **64**, 1967 (1990).
21. V.E. Dmitrienko, V.A. Belyakov, *Pis'ma Zh. Tekh. Fiz.* **6**, 1440 (1980); *Sov. Tech. Phys. Lett.* **6**, 621 (1980).
22. T. Ishikawa, K. Hirano, S. Kikuta, *J. Appl. Cryst.* **24**, 982 (1991).
23. T. Ishikawa, K. Hirano, K. Kanzaki, S. Kikuta, *Rev. Sci. Instrum.* **66**, 1540 (1995).
24. C. Gilès, C. Malgrange, J. Goulon, C. Vettier, F. De Bergevin, A. Freund, P. Elleaume, E. Dartyge, A. Fontaine, C. Giorgetti, S. Pizzini, *Proc. SPIE* **2010**, 136 (1993).
25. J. Goulon, C. Malgrange, C. Gilès, C. Neumann, A. Rogalev, E. Moguiline, F. De Bergevin, C. Vettier, *J. Synchrotron Rad.* **3**, 272 (1996); *Phys. Rev. B* **52**, 10681 (1995).
26. M. Born, E. Wolf, *Principles of Optics*, 6th edn. (Pergamon Press, 1985), pp. 546-547.
27. R.M.A. Azzam, N.M. Bashara, *Ellipsometry and Polarized Light* (North Holland Personal Library, Elsevier Science Publishers, B.V., 1989), pp. 62-63.
28. C.A. Emeis, L.J. Oosterhoff, *Chem. Phys. Lett.* **1**, 129 (1967).
29. J.P. Riehl, F. Richardson, *Chem. Rev.* **86**, 1 (1986).
30. J.P. Riehl, F. Richardson, *J. Chem. Phys.* **65**, 1011 (1976).
31. C. Gauthier, I. Ascone, J. Goulon, R. Cortès, J.M. Barbe, R. Guillard, *Chem. Phys. Lett.* **147**, 165 (1990).
32. M. Born, K. Huang, *Dynamical Theory of Crystal Lattices* (Clarendon, Oxford, 1954), pp. 336-338.
33. D.F. Nelson, *J. Opt. Soc. Am.* **B6**, 1110 (1989).
34. W.F. Brown, S. Shtrikman, D. Treves, *J. Appl. Phys.*, 1233 (1963).
35. R.R. Birss, R.G. Shrubbsall, *Philos. Mag.* **15**, 687 (1967).
36. R.M. Hornreich, S. Shtrikman, *Phys. Rev.* **171**, 1065 (1968).
37. B.B. Kritchetsov, V.V. Pavlov, R.V. Pisarev, V.N. Gridnev, *J. Phys.-Cond. Matter* **5**, 8223 (1993).